

## Epitaxy of Ce and Ce oxides on V(110)

B. Kierren, T. Gourieux, F. Bertran, and G. Krill\*

*Laboratoire de Physique du Solide, Université de Nancy I, Boîte Postale 239, 54506 Vandoeuvre-lès-Nancy, France*

(Received 23 March 1993)

Epitaxial Ce layers have been obtained by evaporation on a V(110) surface. The Ce phase reported some years ago for this system is not confirmed in our experiments: the analysis of reflection high-energy electron-diffraction and x-ray-photoemission data leads us to identify the epitaxial Ce phase with a Ce- $\gamma$  phase. Under several circumstances, epitaxy of Ce oxides has been observed on V(110): in these cases, the epitaxial surface lattice is found to be hexagonal with a parameter  $a_s = 3.9 \pm 0.1 \text{ \AA}$ , and does not depend (in the limit of experimental errors) on the amount of oxygen.

### I. INTRODUCTION

Among all the rare-earth elements, Ce appears to be a very special case because of the possibility of obtaining either a localized or a delocalized character of the  $4f$  electrons in many Ce systems. The well-known isostructural  $\gamma$ - $\alpha$  phase transition in metallic Ce (Ref. 1) is in direct connection with such a property. A drastic reduction (from 5.16 to 4.79  $\text{\AA}$ ) of the lattice parameter occurs during this transition.<sup>2</sup> The idea that this transition may be stimulated by epitaxial growth (via the substrate strains) is of interest in order to have a more comprehensive picture of the description of  $\alpha$  and  $\gamma$  phases, which is still being debated.<sup>3,4</sup>

Recently, Gu *et al.*<sup>5</sup> reported such a transition for a Ce monolayer deposited on a W(110) substrate: as the Ce coverage increased, the lattice parameter of the hexagonal Ce layer decreased, starting from that of a (111)  $\gamma$ -like plane for the half monolayer, up to that of a (111)  $\alpha$ -like plane. Moreover, Homma *et al.* reported some years ago<sup>6,7</sup> the possible growth of a metastable phase of Ce(111) when it is deposited on a V(110) surface at 350°C.<sup>7</sup> From structural data, the authors determined this new Ce\* phase as a trigonal phase, with an in-plane parameter close to that of the  $\alpha$  phase but an out-of-plane parameter close to that of the  $\gamma$  phase. The epitaxial orientation was found to be equally unusual with  $[0\bar{1}1]_{\text{Ce}^*} \parallel [\bar{1}10]_{\text{V}}$ ; this new orientation has been predicted by recent calculations.<sup>8</sup> As pointed out by Homma *et al.*, electronic properties of this new Ce\* phase had to be explored.

In the following, we report such a study by means of Ce  $3d$  x-ray photoemission experiments. However, both reflection high-energy electron-diffraction (RHEED) and photoemission results showed that the epitaxial Ce phase we obtained was not Ce\*, but the "natural" Ce- $\gamma$  phase.

During our experiments (particularly at the early stages of the Ce evaporation), we equally observed the growth of epitaxial Ce oxide films on the V(110) substrate. Our results may be of interest concerning the field of epitaxial ceramic layers in relation with tunnel junction devices [see for instance Refs. 9 and 10 where CeO<sub>2</sub> epitaxial films have been obtained on a Si(111) substrate].

### II. EXPERIMENT

As in Refs. 6 and 7, because of the high reactivity of vanadium with oxygen, the V(110) surface was obtained by evaporation on a (11 $\bar{2}$ 0) sapphire substrate held at 950°C, rather than using a single crystal. The thickness of the deposited films was in the range 500–1000  $\text{\AA}$ . The initial Volmer-Weber growth of vanadium reported by Homma *et al.*<sup>6,7</sup> has been reproduced in our experiments by the observation of spotty RHEED patterns. Further vanadium depositions led to the appearance of sharp streaks indicating the growth of a two-dimensional V(110) surface. However, after each evaporation, and despite the good residual pressure during the growth ( $10^{-10}$ -mbar range), the observation of extra streaks on the RHEED patterns was systematic. Auger spectra revealed that it was due to oxygen adsorption. Several hours of ion bombardment and annealing were necessary in order to obtain a V(110) surface free of oxygen. More details concerning the epitaxy of vanadium on sapphire are given in Ref. 11.

Evaporations of Ce were made in an ultrahigh vacuum chamber (base pressure less than  $5 \times 10^{-11}$  mbar) by using a W crucible. Inside the chamber, a cryogenic shield cooled to liquid nitrogen allowed us to perform Ce evaporations at pressures less than  $2 \times 10^{-10}$  mbar in all cases. The deposited thicknesses were measured with a water-cooled quartz oscillator having 10% accuracy. Mainly, three Ce thicknesses were investigated: 10, 21, and 42  $\text{\AA}$ . The Ce depositions were made at different rates (varying from 1.5 to 30  $\text{\AA}/\text{min}$ ) and for different substrate temperatures varying from 20 to 550°C. This includes the growth temperature used in Ref. 7 (350°C).

The surface composition, immediately after deposition, was checked by Auger spectroscopy: spectra were taken in the derivative mode with a cylindrical spectrometer. The energy of the incident electron beam was set to 2 keV with an emission current of 2  $\mu\text{A}$ . RHEED patterns were obtained with a 20-keV electron beam under a 1° or 2° incidence. The photoemission experiments have been carried out with nonmonochromatized Mg  $K\alpha$  and Al  $K\alpha$  photon sources; in both cases, the total resolution was estimated to be 1.1 eV.

### Calibration of RHEED patterns

As it is known that the V(110) surface does not reconstruct or relax,<sup>12</sup> the bulk parameter  $a_b = 3.02 \pm 0.01$  Å has been taken as a reference in order to calibrate all our RHEED patterns. Figure 1(a) shows the typical RHEED patterns we obtain for the clean V(110) substrate. Here, azimuths are  $[001]_V$  and  $[\bar{1}\bar{1}3]_V$ . Two other azimuths were equally observed, namely,  $[\bar{1}\bar{1}3]_V$  and  $[1\bar{1}1]_V$ . The measured distance ratios between the streaks agreed with the predicted theoretical values for a bcc (110) surface to within 1% in all cases. Other azimuths were not observed for V(110) because of the azimuthal rotation which is limited to  $120^\circ$  in our experimental setup.

## III. EPITAXY OF Ce OXIDES ON V(110)

### A. RHEED analysis

Epitaxy of oxidized Ce films was obtained at the early stages of our experiments, when the Ce source was not outgassed enough. The observation of well-streaked RHEED patterns [see Fig. 1(b)] on these oxidized films led us to identify the surface structure as a hexagonal one, with the same azimuthal directions as in the case of pure Ce (see below). The in-plane parameter was found

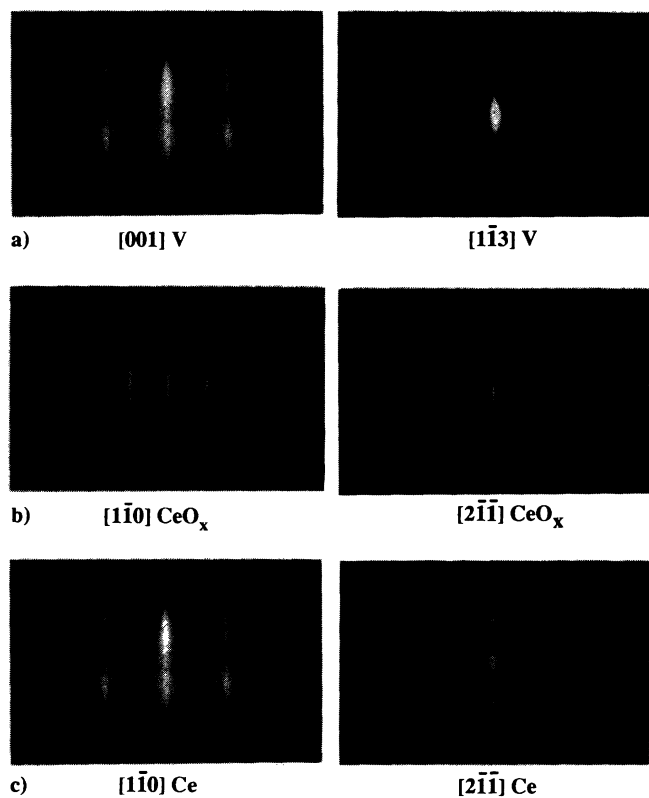
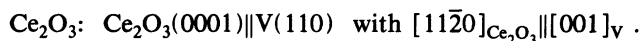
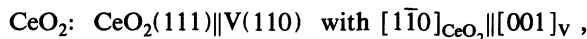


FIG. 1. RHEED patterns: (a) V(110): experimental angular positions are  $15 \pm 1^\circ$  (left) and  $43 \pm 1^\circ$  (right). (b) Oxidized Ce film on V(110) with experimental angular positions  $14 \pm 1^\circ$  (left) and  $47 \pm 1^\circ$  (right). (c) 21-Å Ce on V(110) at room temperature; experimental angular positions are the same as in (b). For convenience, RHEED patterns of epitaxial Ce-oxide films are indexed like a fcc lattice.

to be  $3.9 \pm 0.1$  Å.

Despite the various oxygen quantities present in the oxidized Ce films (as revealed by Auger spectroscopy) between each experiment, the RHEED analysis always gave the same results. This can be explained by the "weak" difference of the hexagonal plane parameters for the mostly known oxide structures [for example,  $CeO_2$ :  $a_{hex} = 5.41/\sqrt{2} = 3.83$  Å (Ref. 2);  $Ce_2O_3$ :  $a_{hex} = 3.89$  Å (Ref. 2)]. In our experiments, we were not able to detect such a difference. For the high-pressure phase CeO, we have  $a_{hex} = 5.09/\sqrt{2} = 3.60$  Å, thus it can be ruled out.

The epitaxial relationships were found to be



As we state here, RHEED experiments alone cannot answer the question of what kind of Ce oxide has grown on the V(110) surface. We will see in the next section that spectroscopic experiments can, at least partially, solve this problem.

### B. Qualitative informations obtained from spectroscopic data

Auger spectra reported in Figs. 2(a) and 2(b) show that a different amount of oxygen was present in the films between each experiment (in fact, it decreased continuously as the Ce source outgassed). From these spectra only, it is not possible to obtain the various oxide concentrations because of the lack, to our knowledge, of any reliable data concerning the relative sensitivity factors between the O(KLL) and the Ce(NVV) Auger peaks.

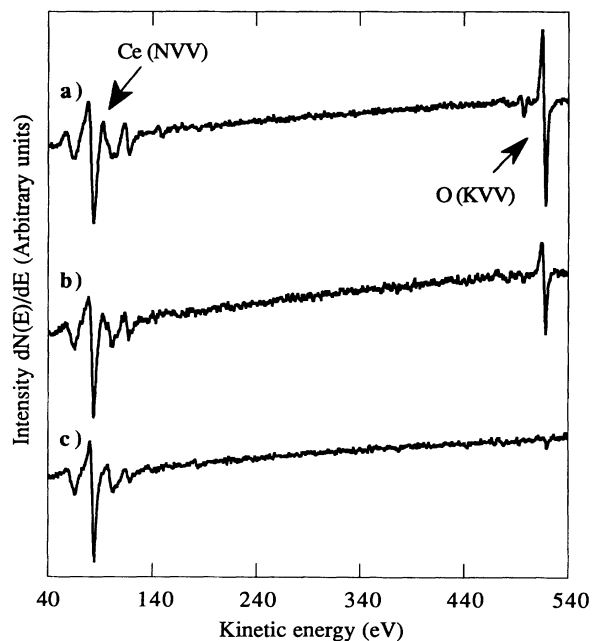


FIG. 2. Derivative Auger spectra in the 40–540-eV kinetic-energy region. (a) and (b) Oxidized epitaxial Ce films with different oxygen concentrations grown on V(110). (c) Clean epitaxial (21-Å) film deposited on V(110).

However, in order to give a preliminary answer to this problem, we focus now on the  $3d$  photoemission data reported in Fig. 3(a), where the  $3d$  XPS spectrum obtained for a low amount of oxygen present in the oxidized Ce film is shown. [see Auger spectrum of Fig. 2(b)]. This spectrum is made of two main contributions corresponding to the two spin-orbit components, each one being divided into two structures which are the well-known  $|4f^1\rangle$  and  $|4f^2\rangle$  final states in the  $3d$  photoemission process of trivalent Ce oxides. As no  $|4f^0\rangle$  final state is observed on this spectrum, we conclude that a trivalent Ce oxide is present. Moreover, the well-screened  $|4f^2\rangle$  channel, which originates from hybridization of  $4f$  orbitals with the oxygen  $2p$  ones, is less intense in our case than for pure  $Ce_2O_3$ .<sup>13</sup> Thus, as the Ce-O phase diagram is only partially known<sup>14</sup> and considering the existence of many nonstoichiometric phases,<sup>15</sup> we suggest that, for this experiment, we obtain an oxygen-deficient epitaxial phase of  $Ce_2O_3$ .

One could expect that epitaxy of tetravalent Ce oxide ( $CeO_2$ ) may occur when the oxygen concentration in the film is higher, as in the case reported in Fig. 2(a). This should be investigated in further photoemission studies.

In order to conclude this section, we summarize the principal results: RHEED and spectroscopic data show that we have obtained epitaxial  $CeO_x$  films on V(110). Epitaxy can be obtained independently of  $x$ , which seems to be a continuous parameter varying with the experimental conditions. Clearly, these conditions and the  $x$  values cannot be derived from our experiments alone.

#### IV. EXPERIMENTAL RESULTS FOR A CLEAN Ce/V(110) INTERFACE

The preparation of Ce layers free of impurities (principally oxygen) has been extremely difficult to execute. This was achieved only after a long outgassing of the Ce source (several weeks) and after obtaining a base pressure in the chamber less than  $5 \times 10^{-11}$  mbar. Figure 2(c) shows a typical Auger spectrum of what we call a clean Ce deposit. The oxygen peak, at 518 eV, is always visible,

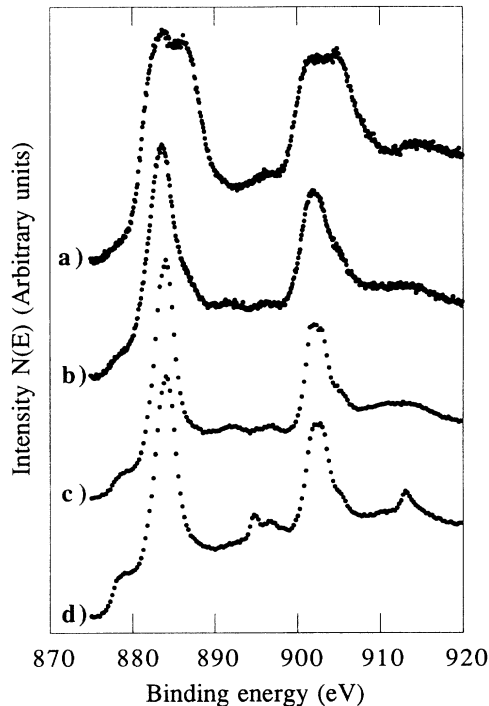


FIG. 3. Ce  $3d$  XPS spectra (Al  $K\alpha$ ) for (a) oxidized epitaxial Ce film corresponding to the Auger spectrum of Fig. 2(a), (b) 21-Å Ce epitaxial film deposited on V(110), (c)  $\gamma$ -Ce from Ref. 17, and (d)  $\alpha$ -Ce from Ref. 17.

but its intensity is very small and comparable to the noise level.

#### A. RHEED analysis

Clean Ce deposits on the V(110) substrate led to the observation of streaks on the RHEED patterns indicating two-dimensional growth. Seven azimuths with three different streak spacings were observed. In Fig. 1(c), two of these azimuths are reported. The good agreement between these data and the expected values for a hexagonal lattice is pointed out in Table I. The in-plane parameter

TABLE I. Experimental angular positions and streak spacing on V(110). The theoretical values refer to a hexagonal lattice.

| Experimental angle ( $\pm 1^\circ$ ) | Theoretical azimuth | $\Delta\phi_{\text{exp}}$ ( $\pm 2^\circ$ ) | $\Delta\phi_{\text{th}}$ | Experimental distance ratio | Theoretical distance ratio |
|--------------------------------------|---------------------|---|--------------------------|-----------------------------|----------------------------|
| $-19^\circ$                          | $[1\bar{2}1]$       | $11^\circ$                                  | $10^\circ, 9$            | $1.53 (\pm 0.08)$           | 1.528                      |
| $-8^\circ$                           | $[2\bar{3}1]$       | $22^\circ$                                  | $19^\circ, 1$            | $2.62 (\pm 0.10)$           | 2.646                      |
| $14^\circ$                           | $[1\bar{1}0]$       | $21^\circ$                                  | $19^\circ, 1$            | $2.62 (\pm 0.10)$           | 2.646                      |
| $35^\circ$                           | $[3\bar{2}1]$       | $12^\circ$                                  | $10^\circ, 9$            | $1.53 (\pm 0.08)$           | 1.528                      |
| $47^\circ$                           | $[2\bar{1}\bar{1}]$ | $11^\circ$                                  | $10^\circ, 9$            | $1.53 (\pm 0.08)$           | 1.528                      |
| $58^\circ$                           | $[3\bar{1}\bar{2}]$ | $20^\circ$                                  | $19^\circ, 1$            | $2.65 (\pm 0.15)$           | 2.646                      |
| $78^\circ$                           | $[10\bar{1}]$       |   |                          |                             |                            |

deduced from the streak spacing is found to be  $3.65 \pm 0.10$  Å: this is the expected value for a (111) plane of Ce- $\gamma$  (3.649 Å). Finally, the angular positions of RHEED patterns showed that the epitaxial relationships are

$$(111)\text{Ce}-\gamma \parallel (110)\text{V} \text{ with } [1\bar{1}0]_{\text{Ce}-\gamma} \parallel [001]_{\text{V}} .$$

This orientation is the usual Nishiyama-Wassermann one, which is commonly encountered for epitaxy of (111)fcc on (110)bcc materials. We note that the same orientation is found for the Ce/W(110) system<sup>5</sup> for which the mismatch is of the same order of magnitude [25% vs 28% for Ce/V(110)].

Despite the change in the Ce evaporation rates (see the experimental details) and/or the substrate temperature, we failed to reproduce the results reported by the authors of Refs. 6 and 7: in all cases, the RHEED analysis led exactly to the same structural results presented above. We mention that for substrate temperatures higher than 450°C, Auger spectra showed that diffusion of oxygen and aluminum arising from the sapphire support occurs through the V film (depending on the V film thickness), after the Ce deposition.

Thus, our conclusions, both for the Ce in-plane parameter and epitaxial orientation of Ce/V(110), are in disagreement with those reported previously by Homma *et al.* However, in the published RHEED patterns from Refs. 6 and 7, fractional-order streaks are apparent for the  $[\bar{1}\bar{1}\bar{1}]_{\text{V}}$  and  $[\bar{1}\bar{1}0]_{\text{V}}$  azimuths. Such structures can be unambiguously associated with the presence of a  $c(6 \times 2)$ -oxygen arrangement on the V(110) surface.<sup>11,12</sup> We recall that the same conclusion has been reached recently for the epitaxy of Nb(110) on a (11 $\bar{2}$ 0) sapphire substrate.<sup>16</sup> Therefore, we suggest that these fractional-order streaks are at the origin of the discrepancy between our results and the conclusions of Homma *et al.*

### B. Photoemission results

The possibility of distinguishing between Ce- $\alpha$  and Ce- $\gamma$  phases with x-ray photoemission has been experimentally and theoretically established for several years.<sup>17,18</sup> Qualitatively speaking, the difference is essentially due to the presence (if  $\alpha$ -Ce) or not (if  $\gamma$ -Ce) of a  $|4f^0\rangle$  contribution to the  $3d$  (or  $4d$ ) spectrum [see Fig. 3(c)].

It is not clear if the Ce trigonal phase reported in Refs. 6 and 7 behaves as an  $\alpha$ -like system, because of the large announced interplane spacing. However, due to the equally large in-plane compression, differences may be observed on a  $3d$  XPS spectrum for this phase when compared to a Ce- $\gamma$  one: indeed, hybridization must occur between the "in-plane"  $4f$  orbitals and the valence band, resulting in a partial delocalization of these  $4f$  states, then leading to the appearance of a  $|4f^0\rangle$  contribution on the  $3d$  and  $4d$  XPS spectra. Recently, it has been pointed out that surface effects occur in  $\alpha$ -like Ce systems,<sup>19,20</sup> leading to a  $\gamma$ -like surface layer. In order to overcome this possible difficulty, we present both  $3d$  and  $4d$  XPS spec-

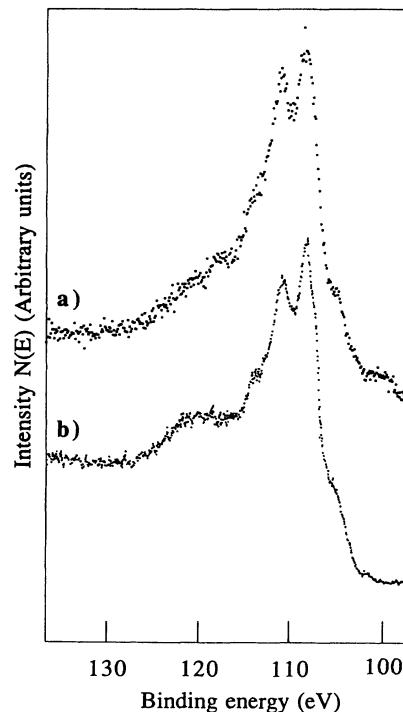


FIG. 4. Ce  $4d$  XPS spectra (Mg  $K\alpha$ ). (a) 21-Å Ce epitaxial film deposited on V(110). (b)  $\gamma$ -Ce after Kowalczyk *et al.* (Ref. 21).

tra for a 21-Å Ce epitaxial deposit: for this thickness we get information both on the surface and the bulk of the Ce film, and the differences in the electron mean free path for  $3d$  and  $4d$  photoemission will point out the eventual differences between the electronic states of the surface and the bulk. As it can be seen in Figs. 3 and 4, these two spectra are typical of a pure Ce- $\gamma$  phase.<sup>17,21</sup> The intensity of the "bump" on the high-binding-energy side of the Ce  $4d$  spectrum is reduced for the case of Ce/V(110) (this is also visible on the  $3d_{3/2}$  line). This bump lies approximately 10 eV from the main lines and can be interpreted as surface and bulk plasmon losses,<sup>22</sup> the intensities of which depend both on surface roughness<sup>22</sup> and thickness of the Ce film.

### V. CONCLUSION

In summary, our experimental results concerning the epitaxy of Ce on V(110) are not in accordance with the conclusions of Homma *et al.* regarding both the epitaxial orientation and the value of the Ce in-plane parameter. At variance with the large uniform compression announced by these authors, we found that the epitaxial Ce phase can be identified with the natural  $\gamma$  phase. Despite the very large lattice mismatch, we note the common Nishiyama-Wassermann epitaxial orientation that occurs in this system. This suggests that geometrical and symmetry properties are of importance, even in these non-matching systems.

We have shown that epitaxial CeO<sub>x</sub> films can grow on

V(110). The in-plane lattice is found to be hexagonal with a parameter  $a_{\text{hex}} = 3.9 \pm 0.1 \text{ \AA}$ . In the limit of our experimental error, it does not depend on the oxygen concentration. This observation can be of interest because it shows that epitaxial compound layers (here  $\text{CeO}_x$ ) can be obtained with controlled concentration on metallic substrates. Finally, the necessity of doing spectroscopic experiments jointly with structural ones has been pointed out.

#### ACKNOWLEDGMENTS

We thank M. Piecuch and S. Andrieu for providing us the sapphire sample, but also for fruitful discussions concerning the interpretation of RHEED data. We are grateful to the Institut de Physique of the University of Neuchâtel for providing us the experimental data of Ref. 17. Our laboratory is "Unité Associée" (URA 155) of the Centre National de la Recherche Scientifique (CNRS).

\*Permanent address: Laboratoire pour l'Utilisation du Rayonnement Synchrotron (LURE), Université de Paris-Sud, Bâtiment 209 D, 91405 Orsay Cedex, France.

- <sup>1</sup>See, for example, D. C. Koskenmaki and K. A. Gschneidner, Jr., *Handbook of the Physics and Chemistry of the Rare Earths*, edited by K. A. Gschneidner, Jr. and L. R. Eyring (North-Holland, Amsterdam, 1978), Vol. 1.
- <sup>2</sup>P. Villars and L. D. Calvert, *Pearson's Handbook of Crystallographic Data for Intermetallic Phases* (American Society for Metals, Metals Park, OH, 1985), Vol. 2.
- <sup>3</sup>O. Eriksson, R. C. Albers, A. M. Boring, G. W. Fernando, Y. G. Hao, and B. R. Cooper, *Phys. Rev. B* **43**, 3137 (1991).
- <sup>4</sup>Y. Baer, M. Grioni, D. Malterre, and W. D. Schneider, *Phys. Rev. B* **44**, 9108 (1991).
- <sup>5</sup>C. Gu, X. Wu, C. G. Olson, and D. W. Lynch, *Phys. Rev. Lett.* **67**, 1622 (1991).
- <sup>6</sup>H. Homma, K. Y. Yang, and I. K. Schuller, *Phys. Rev. B* **36**, 9435 (1987).
- <sup>7</sup>H. Homma, K. Y. Yang, and I. K. Schuller, *Interfaces, Superlattices and Thin Films*, edited by J. D. Dow and I. K. Schuller (Materials Research Society, Pittsburgh, 1987), p. 557.
- <sup>8</sup>S. M. Paik and I. K. Schuller, *Phys. Rev. Lett.* **64**, 1923 (1990).
- <sup>9</sup>H. Koinuma, H. Nagata, T. Tsukahara, S. Gonda, and M. Yoshimoto, *Appl. Phys. Lett.* **58**, 2027 (1991).
- <sup>10</sup>T. Inoue, Y. Yamamoto, S. Koyama, S. Suzuki, and Y. Ueda, *Appl. Phys. Lett.* **56**, 1332 (1990).
- <sup>11</sup>B. Kierren, T. Gourieux, F. Bertran, and G. Krill, *Appl. Surf. Sci.* **68**, 341 (1993).
- <sup>12</sup>D. L. Adams and H. B. Nielsen, *Surf. Sci.* **107**, 305 (1981).
- <sup>13</sup>J. C. Fuggle, M. Campagna, Z. Zołnierak, R. Lässer, and A. Platru, *Phys. Rev. Lett.* **45**, 1597 (1980).
- <sup>14</sup>*Binary Alloy Phase Diagrams*, 2nd ed., edited by T. B. Massalki (American Society for Metals, Metals Park, OH, 1990), Vol. 2.
- <sup>15</sup>M. Gasgnier, G. Schiffmacher, L. Albert, P. E. Caro, H. Dexpert, J. M. Esteva, C. Blancard, and R. C. Karnatak, *J. Less-Common Met.* **156**, 59 (1989), and references therein.
- <sup>16</sup>C. Sürgers and H. V. Löhneysen, *Appl. Phys. A* **54**, 350 (1992).
- <sup>17</sup>E. Wuilloud, H. R. Moser, W. D. Schneider, and Y. Baer, *Phys. Rev. B* **28**, 7354 (1983).
- <sup>18</sup>O. Gunnarsson and K. Schönhammer, *Phys. Rev. B* **28**, 4315 (1983).
- <sup>19</sup>C. Laubschat, E. Weschke, C. Holtz, M. Domke, O. Streble, and G. Kaindl, *Phys. Rev. Lett.* **65**, 1639 (1990).
- <sup>20</sup>C. Laubschat, E. Weschke, M. Domke, C. T. Simmons, and G. Kaindl, *Surf. Sci.* **269/270**, 605 (1992).
- <sup>21</sup>S. P. Kowalczyk, N. Edelstein, F. R. McFeely, L. Ley, and D. A. Shirley, *Chem. Phys. Lett.* **29**, 491 (1974).
- <sup>22</sup>F. P. Netzer, G. Strasser, G. Rosina, and J. A. D. Matthew, *Surf. Sci.* **152/153**, 757 (1985).

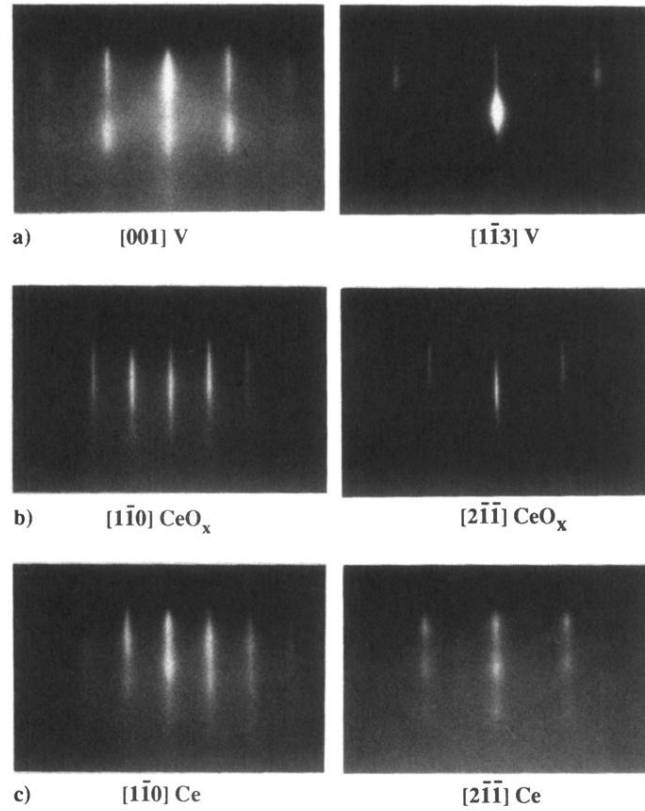


FIG. 1. RHEED patterns: (a) V(110): experimental angular positions are  $15 \pm 1^\circ$  (left) and  $43 \pm 1^\circ$  (right). (b) Oxidized Ce film on V(110) with experimental angular positions  $14 \pm 1^\circ$  (left) and  $47 \pm 1^\circ$  (right). (c) 21-Å Ce on V(110) at room temperature; experimental angular positions are the same as in (b). For convenience, RHEED patterns of epitaxial Ce-oxide films are indexed like a fcc lattice.